



Paul trap experiment to simulate intense nonneutral beam propagation through a periodic focusing field configuration

Ronald C. Davidson*, Philip C. Efthimion, Richard Majeski,
Hong Qin, Gennady Shvets

Plasma Physics Laboratory, Princeton University, Princeton, NJ 08543, USA

Abstract

This paper describes the design concept for a compact Paul trap experimental configuration that fully simulates the collective processes and nonlinear transverse dynamics of an intense charged particle beam that propagates over large distances through a periodic quadrupole magnetic field. To summarize, a long nonneutral plasma column ($L \gg r_p$) is confined axially by applied DC voltages $\hat{V} = \text{const.}$ on end cylinders at $z = \pm L$, and transverse confinement is provided by segmented cylindrical electrodes (at radius r_w) with applied oscillatory voltages $\pm V_0(t)$ over 90° segments. Because the transverse focusing force is similar in waveform to that produced by a discrete set of periodic quadrupole magnets in a frame moving with the beam, the Paul trap configuration offers the possibility of simulating intense beam propagation in a *compact* experimental facility. The nominal operating parameters in the experimental design are: barium ions ($A = 137$); plasma column length $2L = 2$ m; wall radius $r_w = 10$ cm; plasma radius $r_p = 1$ cm; maximum wall voltage $\hat{V}_0 = 400$ V; end electrode voltage up to $\hat{V} = 500$ V; and voltage oscillation frequency $f_0 = 1/T = 60$ kHz. © 2001 Elsevier Science B.V. All rights reserved.

Keywords: Ion beam; Space charge; Stability; Transport

1. Introduction

Periodic focusing accelerators and transport systems [1–5] have a wide range of applications ranging from basic scientific research in high energy and nuclear physics, to applications such as spallation neutron sources, tritium production, heavy ion fusion, and nuclear waste treatment, to mention a few examples. Of particular interest, at the high beam currents and charge densities of practical interest, are the combined effects of the applied focusing field and the intense self-fields

produced by the beam space charge and current on determining detailed equilibrium, stability, and transport properties [1–5]. Through basic experimental studies, analytical investigations based on the nonlinear Vlasov–Maxwell equations, and numerical simulations using particle-in-cell models and nonlinear perturbative simulation techniques, considerable progress has been made in developing an improved understanding of the collective processes and nonlinear beam dynamics characteristic of high-intensity beam propagation [6–14] in periodic focusing and uniform focusing transport systems. Nonetheless, it remains important to develop an improved basic understanding of the nonlinear dynamics and collective processes in

*Corresponding author. Fax: +1-609-243-2749.

E-mail address: rdavidson@pppl.gov (R.C. Davidson).

periodically focused intense charged particle beams, with the goal of identifying operating regimes for stable (quiescent) beam propagation over hundreds, even thousands, of lattice periods of the periodic focusing magnetic field, including a minimum degradation of beam quality and luminosity. High-intensity accelerator systems and beam transport lines are typically large physically and expensive to operate. The purpose of this paper is to describe the design concept for a compact Paul experimental trap configuration that fully simulates the collective processes and nonlinear transverse dynamics of an intense charged particle beam propagating through a periodic quadrupole magnetic field configuration. The idea of using a single-species trap to model periodically focused beam propagation has been discussed by Davidson et al. [15], and by Okamoto and Tanaka [16], although the emphasis of their work is on solenoidal confinement [16], whereas the present paper focuses on periodic quadrupole confinement [15].

The equivalence of the Paul trap configuration to intense beam propagation through a periodic focusing quadrupole field is discussed in Section 2, and in Section 3 we describe the experimental design concept.

2. Paul trap simulator configuration

In practical accelerator applications, if the spacing between quadrupole magnets corresponds (for example) to $S = 2$ m, and the transverse nonlinear beam dynamics is to be followed in detail for 500 lattice periods, then the length of the transport system that is required is 1 km. The obvious question arises as to whether or not it is possible to *model* the nonlinear transverse beam dynamics in a *compact* laboratory configuration. The answer is *yes*, and the key is to recognize that the particle motion in the frame of the beam is nonrelativistic, and that the oscillatory quadrupole focusing force can be simulated in the laboratory frame by applying oscillatory voltages to cylindrical electrodes in a modified Paul trap [15] as illustrated in Fig. 1. A Paul trap [17–22] utilizes oscillatory voltages applied to external electrodes

to provide transverse confinement of the nonneutral plasma in the x – y plane.

To model an axially continuous charged particle beam (or a very long charge bunch), we consider a long nonneutral plasma column [Fig. 1(a)] with length $2L$ and characteristic radius $r_p \ll L$, confined axially by applied DC voltages $\hat{V} = \text{const.}$ on end cylinders at $z = \pm L$. The particles making up the (nonrelativistic) nonneutral plasma in Fig. 1(a) have charge q and mass m . With regard to transverse confinement of the particles in the x – y plane, segmented cylindrical electrodes (at radius r_w) have applied oscillatory voltages $\pm V_0(t)$ over 90° segments with the polarity illustrated in Fig. 1(b). Here, the applied voltage $V_0(t)$ is oscillatory with [15]

$$V_0(t+T) = V_0(t), \quad \int_0^T dt V_0(t) = 0 \quad (1)$$

where $T = \text{const.}$ is the period, and $f_0 = 1/T$ is the oscillation frequency. While different electrode shapes will result in an oscillatory quadrupole potential near the cylinder axis, the configuration shown in Fig. 1(b) is particularly simple and amenable to direct calculation. Neglecting end effects ($\partial/\partial z = 0$), and representing the applied electric field by $\mathbf{E}_a = -\nabla_\perp \phi_a(x, y, t)$, where $\nabla_\perp \cdot \mathbf{E}_a = 0$ and $\nabla_\perp \times \mathbf{E}_a = 0$, it is readily shown that the solution to $\nabla_\perp^2 \phi_a(x, y, t) = 0$ that satisfies the appropriate boundary conditions at $r = r_w$ in Fig. 1(b) is given near the axis ($r \ll r_w$) by [15]

$$q\phi_a(x, y, t) = \frac{1}{2}m\kappa_q(t)(x^2 - y^2) \quad (2)$$

where the oscillatory quadrupole focusing coefficient $\kappa_q(t)$ is defined by

$$\kappa_q(t) \equiv \frac{8qV_0(t)}{m\pi r_w^2}. \quad (3)$$

From Eqs. (1) and (3), note that $\kappa_q(t+T) = \kappa_q(t)$ and $\int_0^T dt \kappa_q(t) = 0$. Moreover, $\kappa_q(t)$ has dimensions of $(\text{time})^{-2}$. Most importantly, the leading-order correction [15] to Eq. (2) is of order $(1/3)(r/r_w)^4$. Therefore, for example, if the characteristic radial dimension r_p of the plasma column in Fig. 1 satisfies $r_p/r_w \lesssim 0.1$, then the corrections to the simple quadrupole potential in Eq. (2) are smaller than one part in 10^4 over the transverse region occupied by the plasma particles.

We now construct the Hamiltonian for the transverse particle motion in Fig. 1, neglecting axial variations ($\partial/\partial z = 0$). Denoting the (dimensional) transverse particle velocities by $\dot{x} = dx/dt$ and $\dot{y} = dy/dt$, and the self-field electrostatic potential due to the plasma space charge by $\phi_s(x, y, t)$, it readily follows that the Hamiltonian $H_{\perp}(x, y, \dot{x}, \dot{y}, t)$ describing the transverse particle motion is given by

$$H_{\perp}(x, y, \dot{x}, \dot{y}, t) = \frac{1}{2}m(\dot{x}^2 + \dot{y}^2) + \frac{1}{2}m\kappa_q(t)(x^2 - y^2) + q\phi_s(x, y, t), \quad (4)$$

where use has been made of Eq. (2). Consistent with Eq. (4) and Fig. 1, we summarize here the nonlinear Vlasov–Poisson equations describing the self-consistent evolution of the distribution function $f(x, y, \dot{x}, \dot{y}, t)$ and self-field electrostatic potential $\phi_s(x, y, t)$ in the transverse phase space (x, y, \dot{x}, \dot{y}) . Of course, the characteristics of the nonlinear Vlasov equation correspond to the single-particle orbit equations calculated from Eq. (4), with $d\mathbf{x}_{\perp}/dt = m^{-1} \partial H_{\perp} / \partial \dot{\mathbf{x}}_{\perp}$ and $d\dot{\mathbf{x}}_{\perp}/dt = -m^{-1} \partial H_{\perp} / \partial \mathbf{x}_{\perp}$. It readily follows that the nonlinear Vlasov–Poisson equations consistent with the Hamiltonian in Eq. (4) can be expressed as

$$\left\{ \frac{\partial}{\partial t} + \dot{x} \frac{\partial}{\partial x} + \dot{y} \frac{\partial}{\partial y} - \left(\kappa_q(t)x + \frac{q}{m} \frac{\partial}{\partial x} \phi_s \right) \frac{\partial}{\partial \dot{x}} - \left(-\kappa_q(t)y + \frac{q}{m} \frac{\partial}{\partial y} \phi_s \right) \frac{\partial}{\partial \dot{y}} \right\} f_b = 0 \quad (5)$$

and

$$\left(\frac{\partial^2}{\partial x^2} + \frac{\partial^2}{\partial y^2} \right) \phi_s = -4\pi q \int d\dot{x} d\dot{y} f \quad (6)$$

where $n(x, y, t) = \int d\dot{x} d\dot{y} f$ is the particle number density.

For the intense beam system being simulated, we consider a thin, intense charged particle beam with characteristic radius r_b and average axial momentum $\gamma_b m_b \beta_b c$ propagating in the z -direction through a periodic focusing quadrupole magnetic field with axial periodicity length S . Here, $r_b \ll S$ is assumed, $(\gamma_b - 1)m_b c^2$ is the directed axial kinetic energy of the beam particles, $\gamma_b = (1 - \beta_b^2)^{-1/2}$ is the relativistic mass factor, $V_b = \beta_b c$ is the average axial velocity, q_b and m_b are the particle charge and rest mass, respectively, and c is the speed of

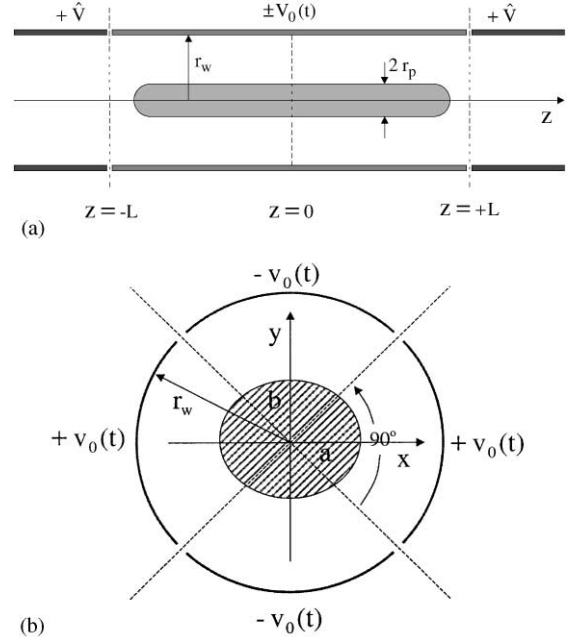


Fig. 1. (a) Axial confinement of a long ($L \gg r_p$) nonneutral plasma column is provided by applied DC voltages $\hat{V} = \text{const.}$ on end cylinders at $z = \pm L$; (b) Transverse confinement of the nonneutral plasma column is provided by cylindrical electrodes at $r = r_w$ with applied oscillatory voltages $\pm V_0(t)$ over 90° segments with $V_0(t + T) = V_0(t)$ and $\int_0^T dt V_0(t) = 0$.

light in vacuo. In addition, the particle motion in the beam frame is assumed to be nonrelativistic. We introduce the scaled time variable $s = \beta_b ct$, and the (dimensionless) transverse velocities $x' = dx/ds$ and $y' = dy/ds$. Then, within the context of the assumptions summarized above, the nonlinear beam dynamics in the transverse, laboratory-frame phase space (x, y, x', y') is described self-consistently by the nonlinear Vlasov–Maxwell equations for the distribution function $f_b(x, y, x', y', s)$ and the space-charge potential $\phi_s(x, y, s)$. For a thin beam ($r_b \ll S$), the transverse focusing force on a beam particle produced by the periodic quadrupole field can be approximated over the cross-section of the beam by [1,3,14]

$$\mathbf{F}_{\text{foc}} = -\kappa_q(s)[x\hat{\mathbf{e}}_x - y\hat{\mathbf{e}}_y] \quad (7)$$

where (x, y) is the transverse displacement of a particle from the beam axis, and the s -dependent

focusing coefficient $\kappa_q(s+S) = \kappa_q(s)$ is defined by

$$\kappa_q(s) = \frac{q_b B'_q(s)}{\gamma_b m_b \beta_b c^2}. \quad (8)$$

Here, the field gradient $B'_q(s)$ is defined by $B'_q(s) = (\partial B_x^q / \partial y)_{(0,0)} = (\partial B_y^q / \partial x)_{(0,0)}$. Note from Eq. (8) that $\kappa_q(s)$ has the dimensions of $(\text{length})^{-2}$, and from Eq. (7) that F_{foc} has the dimensions of $(\text{length})^{-1}$.

The striking feature of the transverse Hamiltonian and nonlinear Vlasov–Poisson equation in Eqs. (4)–(6), valid for the Paul trap configuration in Fig. 1, is that they are identical in form to the corresponding equations describing the transverse dynamics of an intense nonneutral beam propagating through a periodic quadrupole magnetic field [1,3,14] provided we make the replacements

$$t \rightarrow s, \quad m \rightarrow \gamma_b m_b \quad (x, y) \rightarrow (x', y')$$

$$\frac{q}{m} \phi_s(x, y, t) \rightarrow \frac{q_b}{\gamma_b^3 m_b \beta_b^2 c^2} \phi_s(x, y, s)$$

$$\kappa_q(t) [\text{Eq. (3)}] \rightarrow \kappa_q(s) [\text{Eq. (8)}] \quad (9)$$

in the nonlinear Vlasov equation (5), and $\int dx' dy' f \rightarrow \int dx' dy' f_b$ in Poisson's equation (6). Because the transverse focusing force is similar in waveform to that produced by a discrete set of periodic quadrupole magnetics *in a frame moving with the beam*, the Paul trap configuration offers the possibility of simulating intense beam propagation over large distances in a compact experimental facility. The Paul trap configuration considered here is intended to simulate continuous beam propagation in a periodic focusing transport line. In this regard, it is important that the trapped plasma be sufficiently long ($L \gg r_p$) that the characteristic bounce frequency for axial motion in Fig. 1 be much smaller than the characteristic transverse oscillation frequency in the applied oscillatory voltage $V_0(t)$.

The Hamiltonian in Eq. (4) and the nonlinear Vlasov–Poisson equations (5) and (6) describe only the transverse dynamics of the long nonneutral plasma column ($L \gg r_p$) in Fig. 1, and z -variations and axial particle motions are not included in the description. While such a model is expected to provide a good description of the transverse

dynamics of the plasma column for $L \gg r_p$, there are important limitations on the range of applicability [15] of the Paul trap analogy for simulating the propagation of a continuous beam through a periodic focusing lattice. Most importantly, the nonneutral plasma column illustrated in Fig. 1 is confined axially, and the particles execute axial bounce motion between the ends of the plasma column (at $z = \pm L$). If we denote the characteristic thermal speed of a particle by v_{Th} (assumed for present purposes to be similar in the axial and transverse directions), then the characteristic bounce frequency for the axial motion of a particle is $\hat{\omega}_z = 2\pi/T_z$, where $T_z \sim 4L/v_{\text{Th}}$ is the period. We denote the characteristic oscillation frequency for transverse particle motion in the oscillatory quadrupole potential by $\hat{\omega}_q = 2\pi/T_q$ (see Section 3), where T_q is the period for transverse motion. At low-to-moderate density, the period T_q and characteristic plasma radius r_p are related approximately by $T_q \sim 2r_p/v_{\text{Th}}$. Therefore, in an approximate sense, the transverse and axial oscillation frequencies and periods stand in the ratio $\hat{\omega}_z/\hat{\omega}_q = T_q/T_z \sim r_p/2L \ll 1$ (by assumption). On a time scale $t \sim T_z$, the (finite-length) effects of the axial bounce motion of particles in the Paul trap configuration illustrated in Fig. 1 may become important, and limit the validity of the Paul trap analogy with the propagation of a continuous beam through a periodic quadrupole lattice. For sufficiently large $L \gg r_p$, however, the axial bounce period T_z can be very long. As illustrative parameters, consider the case where $r_p = 1$ cm, $2L = 200$ cm, and the frequency $f_0 = 1/T$ of the applied oscillatory voltage $V_0(t)$ is $2\pi f_0 = 4\hat{\omega}_q$. In this case, $T_z \sim 200T_q \sim 800T$, where T is the oscillation period of $V_0(t)$. In this case, a typical particle in Fig. 1 experiences the effects of 800 oscillation periods of the quadrupole focusing potential (800 equivalent lattice periods) before it executes one axial bounce in the trap. For small values of r_p/r_w , the nonlinear image charge force are small compared to the high-fill-factor induction linacs envisioned for heavy ion fusion. Therefore, to simulate such systems with the Paul trap simulator, it will be necessary to form a moderately large-radius plasma with r_p/r_w in the range 0.3–0.5.

3. Experimental design

3.1. Illustrative operating range

Illustrative examples [15] of oscillatory waveforms for the quadrupole focusing coefficient range from a sinusoidal waveform with $\kappa_q(t) = \hat{\kappa}_q \sin(2\pi t/T)$, where $\hat{\kappa}_q = \text{const.}$ and $T = 1/f_0$ is the oscillation period, to a periodic step-function lattice with maximum amplitude $\hat{\kappa}_q$ and filling factor η . The oscillatory applied potential in Eq. (3) [or, equivalently, in Eq. (8)] typically results in a nonneutral plasma column (or intense charged particle beam) that has a pulsating elliptical cross-section in the x - y plane [1–3,14]. In this regard, it is convenient to denote the on-axis ($r = 0$) plasma density by \hat{n} and the corresponding plasma frequency by $\hat{\omega}_p \equiv (4\pi\hat{n}q^2/m)^{1/2}$. From Eq. (3), we further denote the characteristic angular oscillation frequency $\hat{\omega}_q$ for the transverse motion of a single particle in the (maximum) focusing field by

$$\hat{\omega}_q \equiv |\hat{\kappa}_q|^{1/2} = \left| \frac{8q\hat{V}_0}{\pi m r_w^2} \right|^{1/2} \quad (10)$$

where $\hat{V}_0 = |V_0(t)|_{\text{max}}$ is the maximum applied voltage. Transverse confinement [1–3,14] of the nonneutral plasma by the field requires $\hat{\omega}_p/\sqrt{2} < \hat{\omega}_q$. On the other hand, to avoid the so-called envelope instability [3] associated with an overly strong focusing field, the oscillation frequency f_0 should be several times larger than $\hat{\omega}_q/2\pi$. Combining these inequalities gives $\hat{\omega}_p/\sqrt{2} < \hat{\omega}_q \ll 2\pi f_0$, or equivalently,

$$\frac{1}{\sqrt{22\pi}} \left(\frac{4\pi\hat{n}q^2}{m} \right)^{1/2} < \frac{1}{2\pi} \left| \frac{8q\hat{V}_0}{\pi m r_w^2} \right|^{1/2} \ll f_0. \quad (11)$$

The inequalities in Eq. (11) are expected to assure robust transverse confinement of the plasma particles by the oscillatory voltage in Fig. 1.

Eq. (11) applies to either a single-species pure ion plasma or to a pure electron plasma. For a singly ionized pure ion plasma (ion mass number = A), such as barium or lithium, Eq. (11)

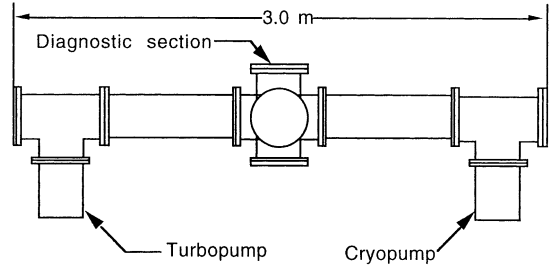


Fig. 2. Elevation view of the Paul Trap Simulator Experiment.

becomes

$$1.49 \times 10^2 \left(\frac{\hat{n}}{A} \right)^{1/2} < 2.5 \times 10^5 \left(\frac{\hat{V}_0}{A r_w^2} \right)^{1/2} \ll f_0 \quad (12)$$

where \hat{n} , \hat{V}_0 , r_w , and f_0 are expressed in units of cm^{-3} , V, cm, and s^{-1} , respectively. As illustrative design parameters for a barium ion plasma ($A = 137$), we take $\hat{V}_0 = 400$ V and $r_w = 10$ cm. Eq. (12) then gives the requirements that $\hat{n} < 1.1 \times 10^7 \text{ cm}^{-3}$, and f_0 exceeding several tens of kHz in order to satisfy the right-most inequality in Eq. (12).

3.2. Experimental design and diagnostics

In this section, we describe in more detail the design concept for a Paul Trap Simulator Experiment (PTSX) being developed at the Princeton Plasma Physics Laboratory (Figs. 2–4). As illustrated in Fig. 2, the apparatus is approximately 3 m in overall length, and consists mainly of a 10" O.D. electropolished stainless-steel chamber with metal-sealed flanges to allow bakeout to 150°C. A centrally located, six-way cross accommodates the laser-induced fluorescence (LIF) diagnostic described later in Section 3.2. Either radial (through the six-way cross) or paraxial (through windows at the axial ends of the device) illumination of the ion population by the excitation laser is possible. The vacuum system consists of a 1000 l/s turbomolecular pump in combination with a cryopump with a rated pumping speed for water of 4000 l/s, with one pump located at either end of the vessel. The

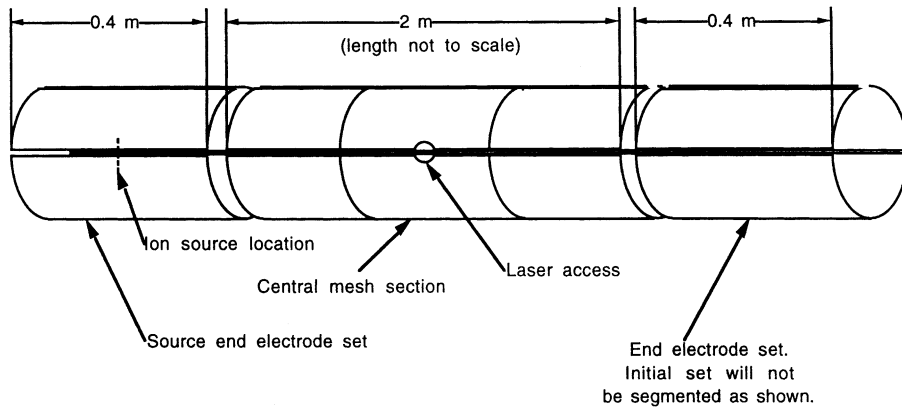


Fig. 3. Electrode arrangement in the Paul Trap Simulator Experiment. Initial operation would utilize a single cylindrical end electrode. A segmented end-electrode permits dumping the ion population for diagnostic purposes, while maintaining good radial confinement as the ions transit the end electrode region into an analyzer.

pumping utilizes “Tee” sections in order to permit good axial access to the device.

The central confinement section of the Paul trap consists of four 200 cm long, azimuthally segmented stainless-steel electrodes which produce the quadrupole fields, as shown in Fig. 3. The diameter of the confining electrode array is 20 cm. In the central section of the trap, the gap between electrodes is locally enlarged to allow passage of a laser beam for the LIF diagnostic. In addition, a section of blackened high-transparency metallic mesh forms the electrodes in this section of the device, to allow imaging of the ion emission without disturbing the electric field configuration. An amplifier powers the electrodes in opposing pairs by means of a step-up transformer with two secondary windings. The amplifier is driven by a programmable waveform generator in order to permit adjustment of the waveform amplitude, pulse shape, and period in real time. A commercial audio amplifier with a low-impedance output (e.g., 3 dB bandwidth, 0.1 Hz–300 kHz, 750 W total output into 4 Ω) is used to drive the electrodes through the step-up transformer to 100–1000 V (peak).

The two end electrode sets in Fig. 3 are different. At the source end, there is a separate 40 cm long set of azimuthally segmented stainless-steel electrodes identical (except in length) to the central electrode set. The barium ion source is located

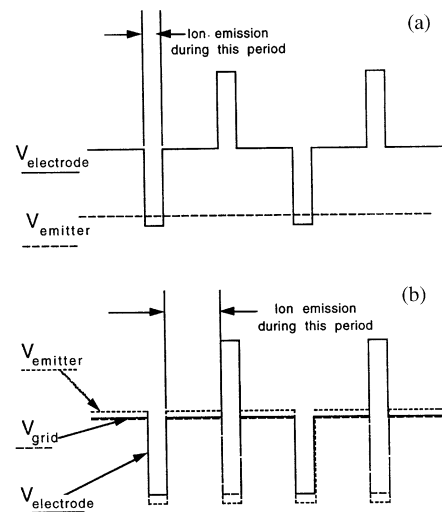


Fig. 4. Electrode potential in the Paul Trap Simulator Experiment. In (a) and (b), the solid lines represent the voltage on two of the four confining electrodes; the remaining two electrodes are excited in phase opposition, as indicated in (b). For the filament ion source, a simple DC bias is applied as shown in (a), and adjusted to produce the necessary ion current. For the gridded, high-current source, the bias arrangement shown in (b) is employed.

midway along the length of this section of the device. At the opposite end is a simple 40 cm long cylindrical electrode. A separate pair of amplifiers power the segmented-source end electrodes,

coupled as in the central electrodes by transformers. In addition, confining biases on the end electrodes are provided by programmable DC power supplies to also permit real-time adjustment and, if desired, gating of the confining potential. For the segmented end-electrode set, the confining bias is applied at the transformer output winding.

The most suitable ion source for the Paul Trap Simulator Experiment is still under investigation. Initial experiments would utilize a simple barium-coated platinum or rhenium filament as an ion source [23], with rhenium being the favored material for good contact ionization efficiency. In this case, the spiral-wound filament is located at the midpoint of the segmented end-electrode section, as shown in Fig. 3. In addition, a high-transparency grid is located in front of the filament, and a reflecting electrode is located behind the filament. Each electrode is separately biased. This system should be adequate for the simulation of low-intensity ion beams. If higher ion fluxes are required than can be supplied by the filament, then a barium-loaded rhenium plate will be substituted for the filament assembly. In this case, the plate will be radiatively heated from behind by a tungsten filament to about 1000°C . This assembly can also be fitted with an accelerating grid approximately 0.5 cm in front of the plate. The development of such a source will be an important prelude to the study of space-charge-dominated systems.

The technique for filling the Paul trap with barium ions envisioned for this experiment is somewhat different from that employed in previous experiments. Confined ions will execute bounce motion in the trap between the end electrode sets. Hence, it is desirable to fill the trap relatively rapidly, in a time comparable to an ion bounce time. For barium ions injected at an energy comparable to the temperature of the hot emitter (0.1 eV), the directed ion velocity is 3.7×10^4 cm/s, and the bounce time is about 11 ms.

In the case of a moderate intensity system, the particle density in the trap will be about 10^6 cm $^{-3}$. Therefore, the total number of particles in the trap will be about 6.3×10^8 for a column radius of 1 cm, so the required ion current is only 9 nA in

order to fill the trap in 11 ms. However, since the segmented electrode set in which the ion source is located is biased with waveforms ranging from sinusoidal to alternating step-function in pulse shape, it is necessary to bias the ion source to near the peak (negative) voltage of the electrode waveform in order to extract ions at a low energy, as shown in Fig. 4. In this case, ions are extracted from approximately one-half the source area during the time that $V_{\text{electrode}} < V_{\text{source}}$, so that the duty factor for ion extraction is $\eta/2$, where η is the filling factor. For $\eta/2 \sim 0.25$, the required peak ion current to fill the trap in 11 ms rises to about 40 nA. For a 2 cm diameter spiral filament source, a very modest difference potential will be enough to overcome space-charge effects and supply the necessary current.

The study of space-charge-dominated systems requires higher ion density. If the maximum particle density required is 10^7 cm $^{-3}$, the total number of particles in the trap will rise to 6.3×10^9 , so the required ion current will rise to 400 nA when the duty factor is included. The required current density is still modest (1.2×10^{-7} A/cm 2) if the source is now a barium-loaded rhenium plate, 2 cm in diameter. A modest (few volt) difference potential between the ion source and the peak electrode voltage would be sufficient to supply the required ion current.

Once the desired number of ions has been loaded into the trap, a DC bias identical to that applied to the cylindrical electrode at the other end of the trap is applied to all four segments of the source end electrodes. The pulsed electrode voltage (if any) is gated off, and the evolution of the confined ion population in the trap can be studied.

There are many ways of detecting ions in a trap. The easiest is to extract the ions from the trap using a high voltage pulse, and then counting them. This destroys the ion population. A non-destructive technique is to measure the ions with laser-induced fluorescence (LIF). The principle of LIF is to excite an electron from a lower energy level to a higher state in an atom or ion with a tunable laser source and to observe the photon emission when it transitions back to a lower energy state. This is a resonant process and the

cross-section for absorption of the laser photon is very high, resulting in low power requirements for the laser pulse. Laser-induced fluorescence is used in many chemistry and physics applications to measure such parameters as particle density, velocity distribution, and electric and magnetic fields [19,24–27].

With the advent of ion Paul traps, some very impressive spectroscopy experiments have been performed using laser-induced fluorescence. The unique (and benign) features for spectroscopic studies in traps are characterized by collision-free storage of a sample, isolated in space and devoid of uncontrollable influences such as collisions with walls or perturbing external fields. Werth [26] has demonstrated the imaging of a single barium ion in a trap. Traps have been proposed as frequency standards. Opto-microwave experiments have examined the line-Q of the ground state hyperfine transitions in alkali-like ions. For beryllium ions, linewidths down to 12 mHz from the Zeeman transition at 292 MHz have been observed. The stability is similar to that obtained with cesium beams. The basic parameter underlying resonant laser excitation is the probability of excitation per particle. The absorption cross-section in the visible region is very large, and a photon density of $N \sim 10^{11} \text{ cm}^{-2} \text{ s}^{-1} \text{ Hz}^{-1}$ is sufficient to saturate the desired state. Consequently, a laser with a spot size of 1/2 mm and less than 1/4 W of power is adequate.

In the Paul Trap Simulator Experiment, it is proposed to use laser-induced fluorescence to diagnose the barium ion plasma microstate, including the ion density profile and the ion velocity distribution parallel and perpendicular to the axis of the trap. Measurements will be carried out in the plane equidistant between the two end electrodes of the trap. By sweeping the frequency of the probing laser across the resonance transition, the velocity distribution parallel to the axis of the plasma column will be measured, because the laser light will be Doppler-shifted. This will be accomplished with a tunable CW dye laser, thereby allowing for a measurement of emittance. The fluorescence light will be measured with a CCD camera and an interference filter looking perpendicular to the laser beam. The CCD camera will

make simultaneous measurements along the chord of the laser beam through the plasma. The intent is to have the volume of measurement to be on the order of a cube with 1 mm side dimensions. The laser light and detector assembly will be translated in order to measure the density profile and the velocity distribution in both directions.

The laser-induced fluorescence measurements will yield the ion density profile of the barium ions, as well as the ion velocity distribution parallel and perpendicular to the axis of the trap. The velocity-space measurements will allow for the study of ion emittance in quadrupole beam transport. By spoiling the waveform of the bias potential of the Paul trap, the effects of beam mismatch on emittance growth and halo particle production can be investigated. Furthermore, sufficiently long integration times will allow for the measurement of the halo particle density profile. Finally, the development of laser-induced fluorescence as a diagnostic to investigate heavy ion beam transport will allow LIF to be applied as a diagnostic tool in heavy ion fusion facilities.

Finally, in the Paul Trap Simulator Experiment, it is proposed to use a high-frequency electric probe to characterize the collective oscillations excited in the plasma. The transverse electric field oscillation is on the order of 30–66 kHz. The oscillating bias voltage applied to the poles of the trap and the ion space-charge potential determine the transverse oscillation frequency. The axial bounce frequency is a function of the distance between the end electrodes and the thermal velocity of the ions. The axial bounce frequency is small (100 Hz) because of the small ion thermal velocity ($3.7 \times 10^4 \text{ cm/s}$). To monitor and characterize these oscillations, the electric field probe is inserted in the trap, and the probe is coupled to a network analyzer to measure the probe frequency spectrum. The collective oscillation frequencies can also be used to estimate the line density and the space-charge potential.

4. Conclusions

The Paul Trap Simulator Experiment and associated diagnostic suite described in Section 3

constitute an enormously flexible facility for simulating a wide range of nonlinear collective processes important in the propagation of intense charged particle beams over large distances. Most importantly, the flexible source geometry and ability to vary the voltage waveform $V_0(t)$, either dynamically or from experiment to experiment, permit detailed studies to be carried out over a wide range of density \hat{n} , average radius r_p , and choice of equivalent waveform for the quadrupole focusing field. Furthermore, the laser-induced fluorescence (LIF) diagnostic capability permits a detailed investigation of the evolution of the density profile, rms column radius, transverse emittance, and velocity distribution function. An important dimensionless parameter s that measures the beam intensity [1] is defined by

$$s \equiv \frac{\hat{\omega}_p^2}{2\hat{\omega}_q^2} \quad (13)$$

where $\hat{\omega}_p$ is the plasma frequency, and $\hat{\omega}_q$ is the effective transverse focusing frequency defined in Eq. (10). In the moderate-intensity beams encountered in high energy and nuclear physics applications [2], the self-field parameter s typically satisfies $s \leq 0.2$, corresponding to emittance-dominated beams which are a few or several Debye lengths in diameter. On the other hand, for the space-charge dominated beams of interest for heavy ion fusion [1,3–5], the self-field parameter s can approach unity, corresponding to a very low transverse emittance, and near balance of the applied focusing force and the repulsive space-charge force. The Paul trap simulator has the capability to investigate collective nonlinear processes for values of the self-field parameter ranging from moderate self-field intensity to very high intensity. Furthermore, the waveform for $V_0(t)$, which simulates the quadrupole focusing magnetic field, can be dynamically varied during an experiment, e.g., slowly varying amplitude at fixed frequency, or slowly varying frequency at fixed amplitude. Experimental studies in such a facility could include detailed investigations of: beam mismatch effects and envelope instabilities; collective wave excitations; chaotic particle dynamics and production of halo particles; mechanisms for

emittance growth; and the effects of distribution function on stability properties.

Acknowledgements

This research was supported by the US Department of Energy.

References

- [1] R.C. Davidson, *Physics of Nonneutral Plasmas*, Addison-Wesley Publishing Co., Reading MA, 1990, and references therein.
- [2] A.W. Chao, *Physics of Collective Beam Instabilities in High Energy Accelerators*, John Wiley and Sons, Inc., New York, 1993.
- [3] M. Reiser, *Theory and Design of Charged Particle Beams*, John Wiley & Sons, Inc., New York, 1994.
- [4] E.P. Lee, J. Hovingh, *Fusion Technol.* 15 (1989) 369.
- [5] See, for example, in: I. Hofmann (Ed.), *Proceedings of the 1997 International Symposium on Heavy Ion Inertial Fusion*, Nucl. Instr. and Meth. Phys. Res. A 415 (1998) 1–508, and references therein.
- [6] R.L. Gluckstern, in: M.R. Tracy (Ed.), *Proceedings of the 1970 Proton Linear Accelerator Conference*, Batavia, IL, National Accelerator Laboratory, Batavia, IL, 1971, p. 811.
- [7] I. Hofmann, L.J. Laslett, L. Smith, I. Haber, *Part. Accel.* 13 (1983) 145.
- [8] J. Struckmeier, I. Hofmann, *Part. Accel.* 39 (1992) 219.
- [9] N. Brown, M. Reiser, *Phys. Plasmas* 2 (1995) 969.
- [10] R.C. Davidson, C. Chen, *Part. Accel.* 59 (1998) 175.
- [11] R.C. Davidson, *Phys. Rev. Lett.* 81 (1998) 991.
- [12] P.H. Stoltz, R.C. Davidson, W.W. Lee, *Phys. Plasmas* 6 (1999) 298.
- [13] A. Friedman, J.J. Barnard, D.P. Grote, I. Haber, *Nucl. Instr. and Meth. Phys. Res. A* 415 (1998) 455.
- [14] R.C. Davidson, H. Qin, P.J. Channell, *Phys. Rev. Special Top. Accel. Beams* 2 (1999) 074401; 3 (2000) 029901.
- [15] R.C. Davidson, H. Qin, G. Shvets, *Phys. Plasmas* 7 (2000) 1020.
- [16] H. Okamoto, H. Tanaka, *Nucl. Instr. and Meth. Phys. Res. A* 437 (1999) 178.
- [17] W. Paul, H. Steinwedel, *Z. Naturforschung A* 8 (1953) 448.
- [18] D.J. Wineland, W.M. Itano, R.S. Vandyck Jr., *Adv. Atom. Mol. Phys.* 19 (1983) 135.
- [19] I. Siemers, R. Blatt, Th. Sauter, W. Neuhauser, *Phys. Rev. A* 38 (1998) 5121.
- [20] J. Walz, S.B. Ross, C. Zimmermann, L. Ricci, M. Prevedelli, T.W. Hänsch, *Phys. Rev. Lett.* 75 (1995) 3257.
- [21] M. Schubert, I. Siemers, R. Blatt, *Appl. Phys. B* 51 (1990) 414.
- [22] *Proceedings of the 1999 Workshop on Nonneutral Plasmas*, Princeton University, 1999, in: J. Bollinger,

- R.C. Davidson, R. Spencer (Eds.), American Institute of Physics Conference Proceedings, Vol. 498, 1999, and references therein.
- [23] R. Blatt, G. Werth, Phys. Rev. A 25 (1982) 1476.
- [24] R.A. Stern, J.A. Johnson III, Phys. Rev. Lett. 34 (1975) 1548.
- [25] R.C. Thomson, Spectroscopy of trapped ions, Advances in Atomic, Molecular, and Optical Physics, Vol. 31, Academic Press, Inc., New York, 1993, p. 631.
- [26] G. Werth, Contemp. Phys. 26 (1985) 241.
- [27] M.G. Raizen, J.M. Gilligan, J.C. Bergquist, W.M. Itano, D.J. Wineland, Phys. Rev. A 45 (1992) 6493.